

# Model-assisted Learning-based Framework for Sensor Fault-Tolerant Building HVAC Control

1<sup>st</sup> Shichao Xu  
Northwestern University  
Evanston, USA  
shichaoxu2023@u.northwestern.edu

2<sup>nd</sup> Yangyang Fu  
Texas A&M University  
College Station, USA  
yangyang.fu@tamu.edu

3<sup>rd</sup> Yixuan Wang  
Northwestern University  
Evanston, USA  
yixuanwang2024@u.northwestern.edu

4<sup>th</sup> Zheng O'Neill  
Texas A&M University  
College Station, USA  
zoneill@tamu.edu

5<sup>th</sup> Qi Zhu  
Northwestern University  
Evanston, USA  
qzhu@northwestern.edu

**Abstract**—As people spend up to 87% of their time indoors, intelligent Heating, Ventilation, and Air Conditioning (HVAC) systems in buildings are essential for maintaining occupant comfort and reducing energy consumption. Those HVAC systems in modern smart buildings rely on real-time sensor readings, which in practice often suffer from various faults and could also be vulnerable to malicious attacks. Such faulty sensor inputs may lead to the violation of indoor environment requirements (e.g., temperature, humidity, etc.) and the increase of energy consumption. While many model-based approaches have been proposed in the literature for building HVAC control, it is costly to develop accurate physical models for ensuring their performance and even more challenging to address the impact of sensor faults. In this work, we present a novel learning-based framework for sensor fault-tolerant HVAC control, which includes three deep learning based components for 1) generating temperature proposals with the consideration of possible sensor faults, 2) selecting one of the proposals based on the assessment of their accuracy, and 3) applying reinforcement learning with the selected temperature proposal. Moreover, to address the challenge of training data insufficiency in building-related tasks, we propose a model-assisted learning method leveraging an abstract model of building physical dynamics. Through extensive numerical experiments, we demonstrate that the proposed fault-tolerant HVAC control framework can significantly reduce building temperature violations under a variety of sensor fault patterns while maintaining energy efficiency.

**Index Terms**—Smart Buildings, Building HVAC control, Data-driven, Fault tolerant control

## I. INTRODUCTION

People spend up to 87% of their time in enclosed buildings nowadays[1]. As Heating, Ventilation, and Air-Conditioning (HVAC) systems control the indoor environment of buildings and have a remarkable impact on occupant comfort, productivity, and physical/mental health, it is important to ensure their performance and reliability. In these systems, sensors, in particular temperature sensors, play a vital role in collecting real-time environment condition and facilitating HVAC applications. However, temperature sensors are not always in normal working condition, and according to [2], temperature sensor errors cause over 1/4 of the variable air volume (VAV) terminal unit faults.

In addition, the sensor reading received by HVAC controllers may also suffer from cyberattacks, as many modern buildings have embedded communication networks for integration and inter-communication between different system components, e.g., BACnet[3], KNX[4]. Moreover, HVAC systems still need to provide services when under faults or attacks, as diagnosing the problems and fixing the sensors often takes a significant amount of time. This highlights the increasing need for developing HVAC controls that can tolerate sensor faults and increase system resilience.

There is extensive literature addressing fault detection and diagnosis in buildings. For instance, [5] introduced a strategy using a learning-based method to detect sensor faults in HVAC systems and diagnose the sources. [6] presented an online strategy based on principal component analysis to detect, diagnose and validate sensor faults in centrifugal chillers. Other approaches were introduced in [7, 8, 9]. However, these works mostly focused on detection and diagnosis, and only a few of them discussed fault tolerance against sensor faults. In fact, many fault-tolerant control approaches for HVAC systems were designed for faults that occur in damper, valve, or fan [10, 11, 12]. There are several recent works on sensor fault-tolerant control in buildings, such as [13, 14]. However, [13] employed a rule-based method (e.g., using sensor reading from the nearest zone), and may not provide sufficient resilience in complex practical scenarios. The work in [14] built a physical model for the building and the sensor faults, and assumed that only one thermal zone would be affected by the sensor fault at a time, which is often not the case in practice. Moreover, developing accurate physical models for building thermal dynamics is a difficult and costly process, and considering sensor faults in such modeling adds even more complexity. Thus, effectively controlling HVAC systems under faulty sensor readings remains an open and challenging problem.

In this work, we develop a sensor fault-tolerant framework for building HVAC control with novel neural network-based learning techniques that also leverage an abstract physical model of the building. Specifically, our framework includes

three major learning-based components. First, as the current raw sensor readings may be faulty, a neural network-based temperature predictor is designed based on historical sensor data to provide an alternative estimation of the true temperature. Then, both temperature proposals (raw sensor reading and the temperature predictor output) are sent to a neural network-based selector, which assesses the two temperature proposals with consideration of the historical trend and selects one deemed more trustworthy. Finally, a deep reinforcement learning (DRL) based HVAC controller takes the chosen temperature as the current system state and applies control actuation. These learning-based techniques together provide a robust HVAC control framework that can maintain desired temperature and reduce energy consumption under sensor faults.

While our machine learning based techniques can remove the need for developing detailed and costly building physical models, they face their own challenges in training data availability. In particular, for a new building, we may have to wait for months to collect enough data for training the learning-based components. To address this challenge, we propose a *model-assisted learning* approach that helps the learning components extract knowledge from an abstract physical model and only requires a limited amount of additional labeled data collected from real buildings for training. There are a number of abstract physical models available in the literature [15, 16]. They require much less effort to develop than the accurate physical models (e.g., those used in EnergyPlus [17]). While they alone are often not accurate enough for building HVAC control, their capturing of the underlying physical laws can guide the learning process for the neural network-based components and significantly improve the learning effectiveness.

To summarize, our work makes the following contributions:

- We present a novel sensor fault-tolerant learning-based framework to achieve sensor fault resilience on building HVAC control. The framework includes three neural network-based components: a temperature predictor that estimates the true temperature, a selector that assesses the predictor output and the raw sensor reading and selects one, and a DRL-based controller that generates the control signal.
- We develop a new method called model-assisted learning that leverages the knowledge from an abstract physical model to enable learning with a small amount of labeled data.
- We conduct a number of experiments on buildings with a single thermal zone and multiple zones, and demonstrate the effectiveness of our fault-tolerant framework under different types of sensor faults. We also highlight how model-assisted learning can improve the learning process.

The rest of the paper is as follows. Section II discusses the related literature. Section III introduces our approach, including the design of the sensor fault-tolerant framework and model-assisted learning. Section IV shows the experiments and related ablation studies. Section V concludes the paper.

## II. RELATED WORK

### A. Building HVAC control

Building HVAC supervisory controllers can be categorized into two groups, *model-based controllers* and *model-free controllers*. Classic model-based HVAC controllers are often developed based on fundamental physics laws (e.g., considering heat transfer and airflow balance). For example, [15] designed a hierarchical control algorithm based on modeling building thermal dynamics as an RC network, which uses resistance and capacitance elements to model the building envelope heat transfer. [16] also used an RC network model and designed a model predictive control (MPC) algorithm for minimizing the building energy consumption. There are other works [18, 19] that use similar abstract physical models. However, While being easy to develop and fast to run, these abstract physical models often suffer from inaccuracy. In contrast, detailed physical models such as EnergyPlus consider complex factors, including building layout, wall materials, light, shading, occupant behaviors, etc. They are much more accurate, but are typically hard to build and slow to run.

Model-free HVAC controllers usually learn control strategies from historical data. In recent years, DRL-based methods have been explored in works such as [20, 21], where techniques such as deep Q-learning (DQN) and asynchronous advantage actor-critic algorithms (A3C) are applied. Methods have also been proposed to learn the DRL parameters by leveraging building simulation tools [22, 23, 24]. In this paper, we combine the strength of both model-free and model-based methods, by developing a learning-based framework with neural network-based components and leveraging abstract physical models to improve the learning process.

### B. Addressing sensor faults in buildings

There has been a number of works in the literature addressing sensor faults in buildings. In [25], a fault detection method based on correlation analysis was proposed for detecting sensor bias or complete failure. [5] proposed a neural network-based strategy with clustering analysis to detect sensor faults in the HVAC system and diagnose the sources. [6] presented an online strategy based on the principal component analysis (PCA) to detect, diagnose and validate sensor faults in centrifugal chillers. Other related investigations can be found in [7, 8, 9, 26, 27, 28]. However, these works focus on fault detection and diagnosis, not fault-tolerant control. There are a few existing works on sensor fault-tolerant control for building HVAC systems, such as [13, 14], but as stated in Section I, they either employ rule-based methods that target limited scenarios or require physical models that are based on restrictive assumptions. In contrast, our learning-based approach provides resilient control in broader and more practical cases.

### C. Learning with limited data and abstract physical model

When dealing with a limited amount of labeled data in training, techniques such as weakly supervised learning [29, 30] and semi-supervised learning [31, 32, 33] are often considered. However, in our case, even obtaining unlabeled data from real

building operations could be a long process. Thus, we leverage the information from abstract physical models such as those in [15, 16] to reduce the data needed for training. This approach is in principle related to model distillation techniques [34, 35] that distill the physical model into a neural network and then fine-tunes the network with available labeled data. However, unlike in the case for those approaches (which focus on domains such as computer vision), there is not enough unlabeled data in the realistic data distribution that can be fed into the model for distillation in our problem. Thus, we propose model-assisted learning to overcome the difficulty and focus on leveraging the abstract physical models to generate better initial points for model find-tuning.

### III. METHODOLOGY

#### A. System model

We adopted a multi-zone building model with the fan-coil system from [20, 36], where there is a building with  $n$  thermal zones, and a fan-coil system is equipped to provide the conditioned air at a given supply air temperature  $T^{air}$  for each thermal zone. The airflow rate in each zone is chosen from multiple discrete levels  $\{f_1, f_2, \dots, f_m\}$ , and corresponding to  $m$  control actions  $a_i$  for each zone  $i$ . With all  $n$  thermal zones, the control action set is denoted as  $A = \{a_1, a_2, \dots, a_n\}$ . In this paper, we denote the current physical time as  $t$ , the ambient temperature, indoor temperature for zone  $i$ , and the control action at time  $t$  as  $T_t^{out}$ ,  $T_t^{in(i)}$ ,  $A_t$ , respectively, and we set  $T_t^{in} = \{T_t^{in(i)} | i \in 1 \dots n\}$ . The system sends current states (indoor and ambient temperatures) to the HVAC system with a period of  $\Delta t_s$  (which is the simulation period on building simulation platform), and the building HVAC controller provides the control signal (supply airflow rates) with a period of  $\Delta t_c$  (which is the control period).

#### B. Sensor fault-tolerant DRL framework

Fig. 1 depicts the overview of our sensor fault-tolerant DRL framework. It includes three parts: a neural network-based temperature predictor for providing an alternative estimation of the indoor temperature is on the left-hand side, the second part in the middle is a proposal selector that assesses the temperature proposals from the raw sensor reading  $T_t^{in}$  and temperature prediction  $T_t^{pre}$  and selects one, and the third part on the right is a DRL-based HVAC controller. With the design of the predictor and the selector, the DRL controller receives a refined temperature reading as part of its inputs and can maintain a stable performance against sensor faults or attacks. The details of each module are introduced in the following sections. Note that all the modules are trained individually and assembled into the framework after training.

1) *Temperature predictor*: The temperature predictor aims to provide a temperature prediction for the current temperature based on the historical sensor readings with possible faults and other system states. Note that we mark the current system state as  $S_t$ , where  $S_t = (t, T_t^{in}, T_t^{out})$ .

Firstly, the temperature predictor is a neural network that consists of five fully-connected layers. Except for the last

layer, all layers are filtered by a ReLU activation function, and all fully-connected layers are sequentially connected. Detailed neuron number setting can be found in Table I. In the test stage of the temperature predictor, the network takes the historical states aligned with the historical control actions (airflow rate) as the data inputs at time  $t$ , and then outputs a current temperature prediction value  $T_t^{pre}$ .

The training data for the predictor network is collected by running a naive ON-OFF controller on the building HVAC system for four days. This can happen in the first several days before the deployment of our framework in most scenarios (e.g., for a new building), and thus we can assume that the collected data will not be polluted by the sensor faults in this short period of time. And we get a (state, action) sequence from  $(S_1, A_1)$  to  $(S_L, A_L)$ . For the convenience of supervised training, we select data sequences

$$\{(S_{t-k}, A_{t-k}), (S_{t-k+1}, A_{t-k+1}), \dots, (S_{t-1}, A_{t-1})\}$$

with length  $k$  and  $t \in [k+1, L]$  from the historical data. These sequences are chosen with an interval  $v$ , which means that  $t \in [k+1, L]$  is selected in the format  $k+1, k+v+1, k+2v+1, \dots$ . The collected data set is used as the training data inputs of the neural network, with the corresponding label  $S_t$  for each data sequence. Then, we train the neural network based on the loss function  $\mathcal{L}_{pre}$  as

$$\mathcal{L}_{pre} = \| (T_t^{pre} + T_{ofs}^{pre}) - T_t \|^2, \quad (1)$$

where  $T_t^{pre}$  is the temperature prediction at time  $t$  from the network's output,  $T_{ofs}^{pre}$  is an estimated offset for bringing the absolute mean value of the neural network's output close to zero, which lowers the difficulty for the neural network learning through the given data sequences. It is a fixed hyper-parameter and defined in Table I.  $T_t$  is the actual indoor temperature, which is the ground truth label. After finishing training, the predictor can take the historical system states containing the raw sensor reading to generate the temperature prediction. We should mention that this historical system states in the test stage may contain faulty sensor readings, while the training data for temperature prediction does not have any faulty data, which is different from the temperature proposal selector we will introduce in the next section. The designing of this training strategy using pure historical data is inspired by our preliminary experiments, which indicated that adding the faulty sensor reading to the training data did decrease the performance on temperature predictions, compared to training with non-faulty data. In other words, the temperature predictor takes benefit from the over-parameterization of neural network as well as the long historical sequence embedded in the input samples, which leads to a rational neural network output even under faulty sensor readings.

2) *Temperature proposal selector*: The temperature proposal selector aims to choose the best candidate from the temperature proposals and send it to the DRL controller for further control steps. We train this module in a self-supervised way, where all the training labels are generated automatically and the objective is to distinguish between the real data and the faulty (fake)

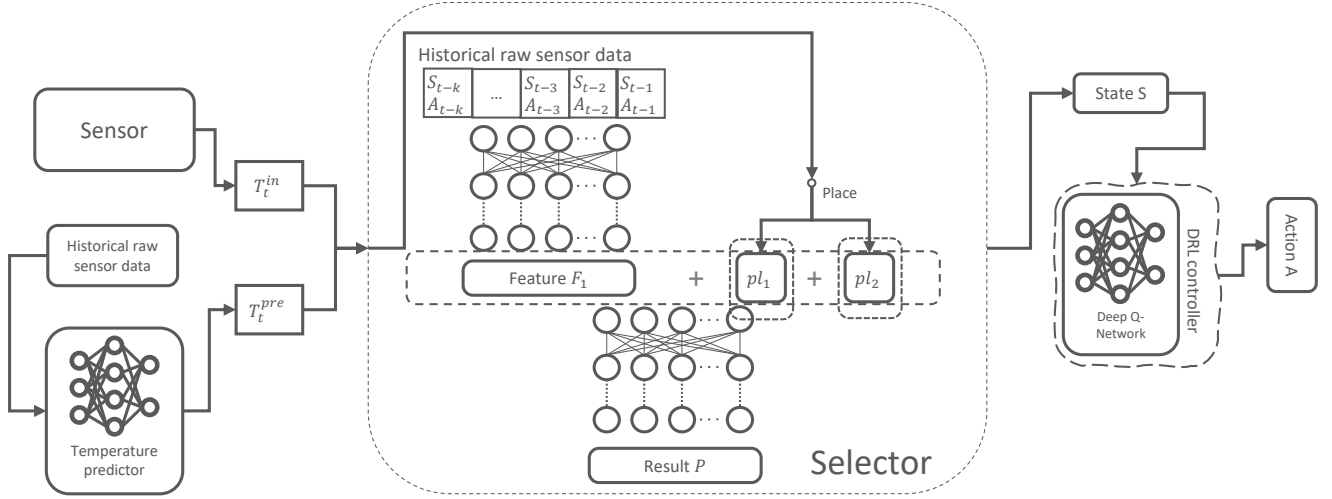


Fig. 1: Overview of our sensor fault-tolerant framework for building HVAC system. There are three main components: two modules providing temperature proposals on the left, a selector in the middle, a DQN-based HVAC controller on the right. The temperature proposals consist of the raw sensor reading  $T_t^{in}$  and the current temperature prediction  $T_t^{pre}$  that comes from the learned temperature predictor, which leverages the historical sensor data. The proposal selector provides a classification result to choose between the predictor output and the raw sensor value. Then, the DRL controller takes the selected temperature proposal and calculates the corresponding control action.

data. Apart from the comparison between the real and fake, we also make the comparison inside the fake data and indicate which one is closer to the actual temperature value. This extra comparison further boosts the proposal selector and helps it address the scenarios with inaccurate temperature proposals.

The temperature proposal selector module is made of a neural network that consists of eight layers. The selector firstly takes the historical system state and the historical control actions  $\langle (S_{t-k}, A_{t-k}), (S_{t-k+1}, A_{t-k+1}), \dots, (S_{t-1}, A_{t-1}) \rangle$  as the part of the network input. Then this historical information will be sent to the first network layer. Including the first layer, there are four sequentially connected one-dimensional convolutional layers with the ReLU activation function on the bottom of the network. The output feature of these layers is two-dimensional in each data sample, and we convert it to a one-dimension feature vector  $F_1$ . Then the rest of the network inputs are two selected temperature proposals, the raw sensor reading  $pl_1$  and the temperature prediction value  $pl_2$ , and they will be concatenated with the feature vector  $F_1$ . As shown in Fig. 1, four fully-connected layers receive features vector  $F_1$  and with those two selected temperature proposals  $pl_1, pl_2$  (note that the first three of them have ReLU activation function). The last fully-connected layer has two neurons, which will be sent to a softmax layer and output a binary classification result by selecting the index with the maximum output value.

Furthermore, the construction of the training data used for the temperature proposal selector differs from the previous module. The historical system state  $S_{t-i} (i \in [1, k])$  and the historical control actions  $A_{t-i} (i \in [1, k])$  are selected from the simulation data which is the same as in Section III-B1. The data in the two temperature proposals contain both correct and

faulty data. So the training data consists of three types:

- Training data:  $\langle \text{historical system states } S_{t-i}, \text{ control actions } A_{t-i}, (i \in [1, k]), \text{ real temperature value, faulty temperature value} \rangle$ .  
Label: (1, 0).
- Training data:  $\langle \text{historical system states } S_{t-i}, \text{ control actions } A_{t-i}, (i \in [1, k]), \text{ faulty temperature, real temperature value} \rangle$ .  
Label: (0, 1).
- Training data:  $\langle \text{historical system states } S_{t-i}, \text{ control actions } A_{t-i}, (i \in [1, k]), \text{ faulty temperature value, faulty temperature value} \rangle$ .  
Label: 1 is assigned to the value that is closer to the real temperature. The other is assigned with 0.

Different from the data construction strategy in the temperature predictor module, the historical system states we utilized include the faulty sensor readings. To be specific, for enhancing the robustness of the temperature proposal selector, we use the historical system states under the independent and identically distributed (IID) faults with occurring probability  $P_{sel}$ . IID faults here mean that the fault can happen at each individual simulation step with probability  $P_{sel}$ . If the fault occurs, it uniformly selects a random number from  $[T_l^{out}, T_u^{out}]$ , which is the upper and lower boundary of the ambient temperature, to replace the original sensor temperature reading. Besides, during constructing these data-label pairs, we sample the faulty temperature three times for each real temperature value in the first and second kind of data-label pair. For the last kind of data-label pair, we sample the faulty temperature data four times for each historical sequence. All faulty temperature readings come

from the IID faults. Finally, we learn the temperature proposal selector network through the cross-entropy loss function. The learning rate  $lr_{sel}$  and training epochs  $l_{sel}$  are specified in Table I.

3) *DRL-based controller for building HVAC system*: Because the thermal zone temperature in the next time step only relies on the observation of the current system state, the building HVAC control can be treated as a Markov decision process. We use a DQN-based DRL method that takes the current state  $S_t^{DRL}$  as inputs, which contain

- Current physical time  $t$ ,
- Current indoor air temperature  $T_t^{in}$ ,
- Current ambient air temperature  $T_t^{out}$ ,
- Current solar irradiance intensity  $Sun_t$ ,
- Weather forecast in the next three time steps.

The weather forecast includes ambient temperature and solar irradiance intensity  $T_{t+1}^{out}, \dots, T_{t+3}^{out}, Sun_{t+1}, \dots, Sun_{t+3}$ , which helps the network capture the trend of the environment. The deep Q-network  $Q$  provides the Q-value estimation of current control actions. The algorithm takes the control action with the maximum Q-value and sends it to the HVAC system.

Furthermore, the goal of this DRL controller is to minimize total energy cost while maintaining indoor temperature within a comfort temperature bound  $[T_l, T_u]$ . The reward function  $R_t$  collected from the control steps is designed accordingly as

$$R_t = \alpha \cdot R_c + \beta \cdot R_v \quad (2)$$

$$R_c = -cost(t-1, A_{t-1}) \quad (3)$$

$$R_v = -\sum_{i=1}^n \max(T_l - T_t^{in(i)}, 0) + \max(T_t^{in(i)} - T_u, 0) \quad (4)$$

where  $\alpha$  and  $\beta$  are the scaling factors.  $R_c$  is the reward of energy cost,  $R_v$  is the reward of temperature violation with respect to comfort temperature bound  $[T_l, T_u]$ .  $cost(t-1, A_{t-1})$  is a price function that gives the money cost of the HVAC system from control time  $t-1$  to  $t$  under control action  $A_{t-1}$ . It is designed based on the local electricity price. Following the definition of the reward function, the update of deep Q-network is defined as

$$Q_{t+1}(S_t^{DRL}, A_t) = Q_t(S_t^{DRL}, A_t) + \eta_0(R_{t+1} + \gamma \max_{A_{t+1}} Q_t(S_{t+1}^{DRL}, A_{t+1}) - Q_t(S_t^{DRL}, A_t)) \quad (5)$$

where  $\eta_0$  is the learning rate for the deep Q-network, and  $\gamma$  is the decay factor of the accumulative reward.

### C. Model-assisted learning

Our sensor fault-tolerant framework has three modules that require neural network training. The performance of a learning model is typically strongly correlated with the amount of available labeled data. However, collecting labeled data from real building operations takes time, which often leads to the problem of training data insufficiency. With the techniques in [37, 38], the training time and the required data of the

DRL control module can be largely reduced. With the special training data construction strategy introduced in Section III-B2, the selector also has sufficient data for training. Thus, we focus our effort on the data insufficiency issue for the temperature predictor. We introduce the model-assisted learning method to combine a limited number of accurately labeled data  $D^L$  with the knowledge we can gain from an abstract physical model  $M$  for the training, as shown in Fig. 2.

Specifically, for each element  $u$  in the neural network input  $s$ , we can define its range based on its physical meaning. Then considering the range for all the elements in  $s$ , we can define a space  $H$  that contains all  $s$  in its range combinations and  $s \in H$ . Note that  $H$  is a space that is much larger than the actual data distribution for network inputs, which means that many unrealistic cases that will never happen in the real world might occur when sampling from  $H$ .

In our model-assisted learning process, the initial step is to collect enough samples from data space  $H$ . However, we notice that the input size of the neural network (temperature predictor),  $(2+2n)k$ , is large. Taking  $n=4, k=20$  for example, the sampling is on a 200-dimensional continuous data space, which is too expensive for simple uniform sampling. Thus, we only sample the first historical state uniformly among that subspace of size  $2+2n$ , and then feed that historical state to the physical model  $M$  to predict the next historical state. Then we generate the latter historical states by repetitively applying the previous historical states to the physical model. In this way, we can collect the sample sequences of length  $k$  and form an input data set  $D$ . We then divide  $D$  into mini-batches and call them random batches  $\{\mathbf{x} | \mathbf{x} \subset D\}$ , and we note the batch size of  $\mathbf{x}$  as  $b$ . In each update step  $i$ , we start from the current network weights  $\Phi_i$ , and select a random batch  $\mathbf{x}$  and apply the abstract physical model  $M$  on them to get the corresponding labels  $\mathbf{y}$ . Next, we are able to get a new model  $\Theta_i$  by updating the parameters on  $\Phi_i$  using the random batch  $\mathbf{x}$  and its corresponding labels  $\mathbf{y}$ , which follows the equation

$$\Theta_i = \Phi_i - \eta_2 \nabla_{\Phi_i} \mathcal{L}_{MSE}(\Phi_i), \quad (6)$$

where  $\mathcal{L}_{MSE}$  is the mean square error loss,  $\eta_2$  is the learning rate. The training lasts for  $n_{iter}$  iterations, and uses a new sampling data batch for each iteration.

Next, we employ accurately labeled data  $D^L$  to further fine-tune the model  $\Theta_i$  from the last step by  $l_{ft}$  epochs, and update to the model weights  $\Theta'_i$ , as described in the following equation

$$\Theta'_i = \Theta_i - \eta_3 \nabla_{\Theta_i} \mathcal{L}_{target}(\Theta_i), \quad (7)$$

where  $\mathcal{L}_{target}$  is the loss function for the target task,  $\eta_3$  is the learning rate for this step.

Looking back to what we have done, we first use the random batch  $\mathbf{x}$  to distill the physical model  $M$  as a pre-trained model for the current step, and then we fine-tune the model using the accurately labeled data. The final performance of model  $\Theta'_i$  should reflect the quality of the initial update from  $\Phi_i$  to  $\Theta_i$ , which depends on the corresponding random batch  $\mathbf{x}$  and the physical model  $M$ 's output knowledge  $\mathbf{y}$ .  $\mathcal{L}_{target}$  shows a reference value considering the improvement brings

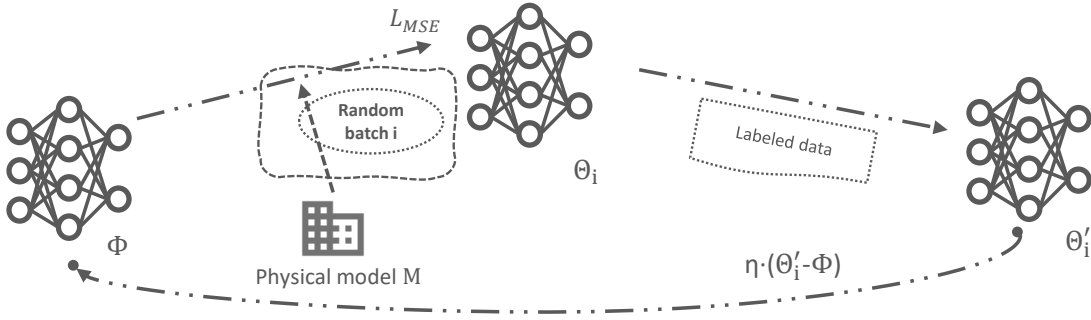


Fig. 2: Overview of our model-assisted learning for training with limited amount of labeled data and a physical model. We use the random batch to extract knowledge from the physical model and form the distilled model. And we apply the labeled train set to fine-tune the model and evaluate using the labeled test set. The feedback will reflect on the random batch to guide the knowledge distillation process.

by the Equation (6) while  $\Theta'_i - \Phi_i$  provides a better updating direction for the current knowledge extraction step compared to the Equation (6). So we determine the true updating step for the initial model  $\Phi_i$  as

$$\Phi_i = \Phi_i - \eta_1(\Theta'_i - \Phi_i) \quad (8)$$

Following this updating steps for  $n_{iter}$  iterations, we then use all the accurately labeled data  $D^L$  to fine-tune the extracted model  $\Phi_i$  to achieve our target model. The fine-tuning step has the learning rate  $\eta_3$  by  $l_{ft}$  epochs.

#### IV. EXPERIMENTAL RESULTS

##### A. Experiment settings

The experiments are run on an Ubuntu OS server equipped with NVIDIA TITAN RTX GPU cards. The learning algorithm implementations are based on the Pytorch framework. The Adam optimizer [39] is utilized for all neural networks' training. We use the EnergyPlus simulation tool to simulate the behavior of real buildings. Note that this is only for experimentation purpose. In practice, our tool will be deployed directly on real buildings with the modules trained on the data collected from those buildings. Moreover, the interaction between the building simulations in EnergyPlus and the Pytorch learning algorithms is implemented through the Building Controls Virtual Test Bed (BCVTB) [40]. We use a single-zone building and a 4-zone building as the target buildings for conducting our experiments, which are visualized in Fig. 3. The building simulation utilizes the summer weather data in August at Riverside, California, USA, which is obtained from the Typical Meteorological Year 3 database [41]. The hyper-parameter settings mentioned in the previous sections are shown in Table I.

##### B. Physical model

This section introduces the abstract physical model used for model-assisted learning. The mass and energy conservation law for a building zone is presented in Equation (9), where the left of the equation represents energy changes in the zone, the first term at the right represents the introduced HVAC energy to the zone, and the second term at the right is the thermal load

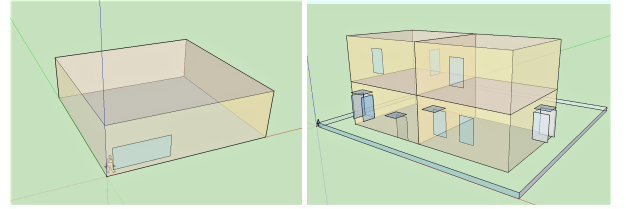


Fig. 3: Rendering of the experimental buildings.

Parameter	Value	Parameter	Value
Temperature-proposal-selector layers	$[2+2n, 512, 256, 128, 256, 256, 2n]$	DQN layers	$[9+n, 50, 100, 200, 400, 16]$
Predictor-layers	$[(2+2n)k, 512, 256, 256, 256, n]$	$T_l$	19 °C
$T_{ofs}^{pre}$	22	$T_u$	24 °C
$l_{ft}$	30	$P_{sel}$	0.3
$\beta$	$6.25e-4$	$\alpha$	$1e-3$
$\eta_2$	$1e-6$	$\eta_1$	$1e-6$
$L$	2880	$\eta_3$	$1e-3$
$\Delta t_s$	1 min	$k$	20
$T_l^{out}$	10 °C	$\Delta t_c$	15 min
$v$	2	$T_u^{out}$	40 °C
$l_{sel}$	50	$l_{r_{sel}}$	$1e-4$
$m$	2	$T^{air}$	10 °C
$\gamma$	0.99	$\eta_0$	0.003
		$b$	32

TABLE I. Hyper-parameters used in our experiments.

in the zone. The thermal load  $\dot{q}_l$  is related to many building system and control parameters such as envelope constructions, internal heat gains, zone air temperature setpoints, etc., which eventually leads to a nonlinear differential equation to solve. For simplification, an abstract model for the zone air temperature dynamics is derived as in Equation (10). This model explicitly relates zone air temperature to system thermal inertia (e.g., historical zone air temperatures), zonal supply air mass flowrate  $\dot{m}$ , outdoor air temperature  $T^{out}$  and estimated modeling error term  $e$ .  $\hat{T}$  and  $T$  are the predicted and measured temperature, respectively.  $m$  is the zone air thermal mass.  $\dot{m}$  is the zonal supply air mass flowrate.  $C_p$  is the zone air specific heat.  $e$  represents an error term. Superscripts *sa*, and *out* are the supply

air, and outdoor air, respectively.  $\alpha$ ,  $\beta$ , and  $\gamma$  are identified coefficients observed from the given short-term historical data.

$$mC_p \frac{dT}{dt} = \dot{m}C_p(T^{sa} - T) + \dot{q}^l \quad (9)$$

$$\hat{T}_{t+1} = \alpha T_t + \beta \hat{m}_{t+1} + \gamma \hat{T}_{t+1}^{out} + e_{t+1} \quad (10)$$

$$e_{t+1} = \sum_{j=0}^{L-1} \frac{\hat{T}_{t-j} - T_{t-j}}{L} \quad (11)$$

### C. Fault patterns and metrics

We consider two types of fault patterns for the sensors in every thermal zone in this paper.

- In the first type of faulty sensor readings, we postulate that the fault happens at each time step with a probability  $p_1$ . Note that the fault can happen in each simulation step, not only on the control steps. If the fault occurs, it uniformly selects a random number from  $[T_l^{out}, T_u^{out}]$  (which is the upper and lower boundary of the ambient temperature at Riverside in our experiments) to replace the original sensor temperature reading. We call this type of faults the IID faults because they have the same probability, same distribution, and independent at each time step.
- For the second type of faulty sensor reading, the fault happens at each time step with a probability  $p_2$ . The difference between it and the former one is that the second fault will last for  $\varpi$  simulation steps and not always happens individually among the time period. Thus this type of fault can cause larger damage to the system than the first one. And we call it continuous faults.

Furthermore, we evaluate the sensor fault-tolerant temperature control results based on the average indoor temperature violation rate  $\theta_i$  for each thermal zone  $i$  and the total energy cost for running the HVAC system. And we evaluate the performance of model-assisted learning on the temperature prediction task with a four-zone building. The measurement for the predictor is based on the root mean square error (RMSE) between the prediction and the actual temperature value.

### D. Sensor fault-tolerant framework

This section shows the performance of our sensor fault-tolerant framework. The experiments are conducted on a single-zone building and a four-zone building under different sensor fault patterns.

1) *Against IID faults:* We first study how much the sensor fault-tolerant framework can protect the control performance from the IID faults. The IID faults happen individually at each simulation step with the probability  $p_1$ , and we test the case where  $p_1$  is chosen from  $[0, 0.1, 0.2, 0.4, 0.6, 0.8]$ . The model is first tested on a single zone building. Table II shows the results comparison between the standard DQN controller (DQN) and our sensor fault-tolerant framework (FTF). We can see that the typical DQN controller's performance significantly deteriorates when facing the IID faults, as the heavily faulty sensor data nearly paralyzed the normal function of the neural network.

The problem gets worse with the fault occurring probability  $p_1$  becomes larger. For our sensor fault-tolerant framework, the average temperature violation rate remains very low under varying degree of IID faults (98.3% to 99.7% reduction in violation rate when compared with standard DQN). Moreover, even with our approach's much more robust control, the energy cost does not increase much, which shows the cost-effectiveness of our sensor fault-tolerant approach.

We also tested our framework on a 4-zone building against the IID faults, and Table III shows its comparison with the standard DQN.  $\theta_1$  to  $\theta_4$  are the temperature violation rate for each of the 4 thermal zones. Again, we can clearly see that our approach can maintain the violation rate at a low level under varying level of sensor faults, and significantly outperform the standard DQN (66.4% to 95.2% reduction in violation rate). It worth mention that when there is no fault, our framework will not introduce additional overhead. Finally, Fig. 4 also provides a visualization of the temperature change on the 4-zone building under IID faults with  $p_1 = 0.4$  with/without the sensor fault-tolerant framework.

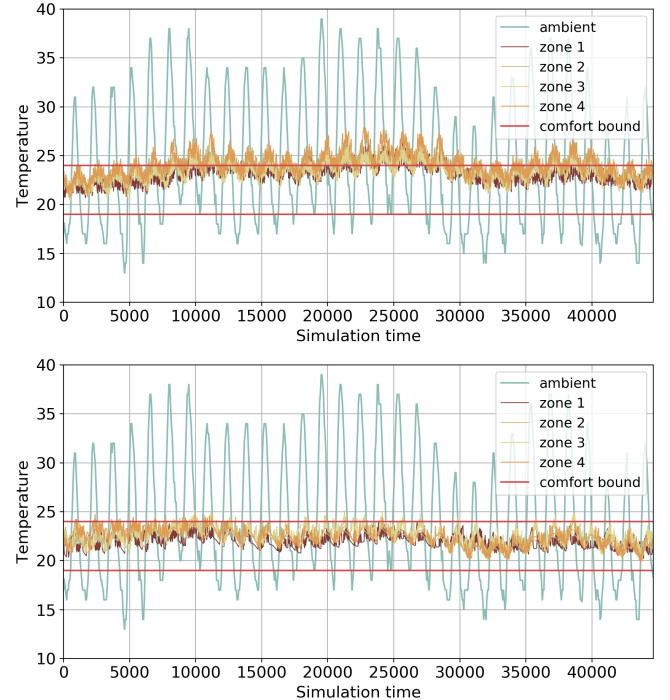


Fig. 4: A visualization of the 4-zone building temperature control under IID faults with  $p_1 = 0.4$  without FTF (above) and with FTF (below).

2) *Against continuous faults:* We then evaluated our approach against continuous faults. Similar to what we have shown in the previous section, the model is tested on a single zone building initially, with the probability  $p_2$  set to 0.4 and  $\varpi$  selected from 0 to 5. The comparison between our approach and the standard DQN is presented in Table IV. The temperature violation rates in this table are all higher than the previous section, which indicates that the continuous faults can cause more damage than the IID faults. As shown in the



	$p_1$	0	0.1	0.2	0.4	0.6	0.8
DQN	$\theta$	0.08	1.18	2.18	3.59	5.90	11.19
	Cost	250.03	245.79	239.74	235.73	228.42	223.22
FTF	$\theta$	0.14	0.02	0.11	0.02	0.01	0.03
	Cost	251.38	253.98	253.22	260.19	268.30	278.23

TABLE II. Comparison between the standard DQN controller and our sensor fault-tolerant framework (FTF) on a single-zone building under the IID faults.  $p_1$  is the fault occurring probability,  $\theta$  is the avg. indoor temperature violation rate (%).

	$p_1$	0	0.1	0.2	0.4	0.6	0.8
DQN	$\theta_1$	0.0	1.68	3.76	14.64	32.18	48.47
	$\theta_2$	0.37	6.27	16.3	30.6	50.70	59.56
	$\theta_3$	1.16	3.17	7.59	15.5	27.22	36.4
	$\theta_4$	1.42	9.33	18.46	28.22	43.50	48.13
	Cost	258.33	246.07	235.17	220.53	197.86	187.76
FTF	$\theta_1$	0.01	0.15	0.12	0.03	0.18	0.33
	$\theta_2$	0.56	2.06	1.55	1.15	1.40	1.94
	$\theta_3$	1.23	3.06	4.54	3.38	3.57	4.58
	$\theta_4$	1.87	1.61	1.83	1.23	1.22	2.43
	Cost	257.36	259.38	263.71	285.34	303.13	302.61

TABLE III. Comparison between the standard DQN controller and our sensor fault-tolerant framework (FTF) on a four-zone building under the IID faults.  $p_1$  is the fault occurring probability,  $\theta_i$  is the avg. indoor temperature violation rate (%) in thermal zone  $i$ .

table, the standard DQN controller cannot maintain effective control under continuous faults, with temperature violation rate increases drastically. In comparison, our approach can effectively maintain the violation rate at a low level (42.9% to 99.4% reduction in violation rate when compared with the standard DQN). We can observe the same trend in Table V, which shows the comparison between our approach and the standard DQN on a four-zone building.

#### E. Evaluation of model-assisted learning

In this section, we conduct experiments on the model-assisted learning algorithm and demonstrate its improvement in the performance of the temperature predictor module. Note that the data only contains non-faulty data in this section for avoiding other factors that may affect the evaluation, which means that there is no sensor fault in both training and testing.

We employ an abstract physical model introduced in Section IV-B for a four-zone building. The abstract model itself has the temperature prediction value with RMSE at 0.832. Then if we only use the accurately labeled data collected from the building to train the neural networks in the temperature predictor module, which is shown in the first block in Table VI

	$\varpi$	0	1	2	3	4	5
DQN	$\theta$	0.08	3.59	6.40	8.33	9.69	9.82
	Cost	250.03	235.73	228.16	227.27	221.77	226.51
FTF	$\theta$	0.14	0.02	3.65	1.76	0.90	1.86
	Cost	251.38	260.19	244.12	249.95	253.37	252.30

TABLE IV. Comparison between the standard DQN controller and our sensor fault-tolerant framework (FTF) on a single-zone building under the continuous faults. The fault lasts for  $\varpi$  steps once it happens,  $\theta$  is the avg. indoor temperature violation rate (%).

	$\varpi$	0	1	2	3	4	5
DQN	$\theta_1$	0	1.68	5.27	9.68	14.41	18.08
	$\theta_2$	0.37	6.27	13.26	21.67	29.57	33.53
	$\theta_3$	1.16	3.17	11.12	14.77	20.05	22.58
	$\theta_4$	1.42	9.33	24.54	34.98	39.54	43.19
	Cost	258.33	246.07	231.42	219.10	213.99	211.20
FTF	$\theta_1$	0.01	0.09	0.06	0.37	0.23	0.54
	$\theta_2$	0.56	1.42	2.05	1.78	2.82	3.51
	$\theta_3$	1.23	4.51	4.22	5.27	6.93	7.85
	$\theta_4$	1.87	1.48	2.49	4.54	6.27	9.37
	Cost	257.36	259.81	268.35	271.89	274.68	272.65

TABLE V. Comparison between the standard DQN controller and our sensor fault-tolerant framework (FTF) on a four-zone building under the continuous faults. The fault lasts for  $\varpi$  steps once it happens,  $\theta_i$  is the avg. indoor temperature violation rate (%) in thermal zone  $i$ .

Model	Samples	RMSE
<i>Labeled data only</i>	360	0.704
<i>Labeled data only</i>	720	0.521
<i>Labeled data only</i>	1440	0.495
<i>Labeled data only</i>	2880	0.369
<i>Distillation + fine-tuning</i>	360	0.711
<i>Distillation + fine-tuning</i>	720	0.516
<i>Distillation + fine-tuning</i>	1440	0.479
<i>Distillation + fine-tuning</i>	2880	0.357
<i>Model-assisted learning</i>	360	0.640
<i>Model-assisted learning</i>	720	0.498
<i>Model-assisted learning</i>	1440	0.465
<i>Model-assisted learning</i>	2880	0.343

TABLE VI. This table shows the experiments on learning the temperature predictor under three different strategies. The first block shows training with labeled data. Then the distillation approach is shown in the second block. Our proposed model-assisted learning shows the best result in the third block.

(the model named *Labeled data only*), we can see that the RMSE remains at the relatively high level, e.g., 0.495 for 1440 data samples, and 0.369 for 2880 data samples. The more labeled data is used, the more accurate the model's prediction is. However, there are only four days of simulation data available with maximum of 2880 data samples for training.

In addition to model-assisted learning, we also test another idea for leveraging the abstract physical model  $M$  to gain better performance, i.e., using the abstract physical model to set initial weights for a neural network, so the network may cost less training data for reaching higher accuracy as it searches from a better initial point. The related technique for obtaining this initial value is model distillation [34]. However, as mentioned earlier, choosing the data to feed the neural network is challenging for distillation. Here we use the same sampling approach as proposed in Section III-C, i.e., sampling from data space  $H$  and feeding the samples  $\mathbf{x}$  to the abstract physical model  $M$ . Then we get the corresponding data pair  $(\mathbf{x}, \mathbf{y})$ , and train the network using  $(\mathbf{x}, \mathbf{y})$  with learning rate  $\eta_2$  for  $n_{iter}$  iterations (a new sampling data batch for each iteration). Next, we fine-tune this newly trained model with learning rate  $\eta_3$  in  $l_{ft}$  epochs on the accurately labeled data. The model obtained in this way is named as *Distillation + fine-tuning* (which is shown in the middle of the Table VI). Finally, we apply our proposed model-assisted learning to leverage the



abstract physical model, and the approach is marked as *Model-assisted learning* in Table VI (the last block). We can observe from the table that, *Distillation + fine-tuning* provides a worse initial point of the network for fine-tuning on only 360 data samples than the randomized initial weights, but it can help the learning when there are more data samples. Most importantly, with the same amount of labeled data, *Model-assisted learning* can achieve better performance than the above two methods, which reaches RMSE 0.465 on 1440 training samples and 0.343 on 2880 training samples.

## V. CONCLUSION

In this paper, we present a novel learning-based sensor fault-tolerant control framework for building HVAC systems against faulty sensor readings, which includes neural network-based components for temperature prediction, temperature proposal selection, and DRL-based HVAC control. We also introduce a model-assisted learning approach that leverages abstract physical model to overcome the difficulty in training data insufficiency. Experimental results demonstrate the effectiveness of our framework and the model-assisted learning method.

## REFERENCES

- [1] N. E. Klepeis, W. C. Nelson, W. R. Ott, J. P. Robinson, A. M. Tsang, P. Switzer, J. V. Behar, S. C. Hern, and W. H. Engelmann, "The national human activity pattern survey (nhaps): a resource for assessing exposure to environmental pollutants," *Journal of Exposure Science & Environmental Epidemiology*, vol. 11, no. 3, pp. 231–252, 2001.
- [2] J. Qin and S. Wang, "A fault detection and diagnosis strategy of vav air-conditioning systems for improved energy and control performances," *Energy and buildings*, vol. 37, no. 10, pp. 1035–1048, 2005.
- [3] H. M. Newman, *BACnet: The Global Standard for Building Automation and Control Networks*. Momentum Press, 2013.
- [4] W. S. Lee and S. H. Hong, "Knx—zigbee gateway for home automation," in *2008 IEEE International Conference on Automation Science and Engineering*. IEEE, 2008, pp. 750–755.
- [5] Z. Du, B. Fan, X. Jin, and J. Chi, "Fault detection and diagnosis for buildings and hvac systems using combined neural networks and subtractive clustering analysis," *Building and Environment*, vol. 73, pp. 1–11, 2014.
- [6] S. Wang and J. Cui, "Sensor-fault detection, diagnosis and estimation for centrifugal chiller systems using principal-component analysis method," *Applied Energy*, vol. 82, no. 3, pp. 197–213, 2005.
- [7] J. C. da Silva, A. Saxena, E. Balaban, and K. Goebel, "A knowledge-based system approach for sensor fault modeling, detection and mitigation," *Expert Systems with Applications*, vol. 39, no. 12, pp. 10977–10989, 2012.
- [8] J. Fonollosa, A. Vergara, and R. Huerta, "Algorithmic mitigation of sensor failure: Is sensor replacement really necessary?" *Sensors and Actuators B: Chemical*, vol. 183, pp. 211–221, 2013.
- [9] W. Kim and S. Katipamula, "A review of fault detection and diagnostics methods for building systems," *Science and Technology for the Built Environment*, vol. 24, no. 1, pp. 3–21, 2018.
- [10] G. P. Henze, D. E. Kalz, C. Felsmann, and G. Knabe, "Impact of forecasting accuracy on predictive optimal control of active and passive building thermal storage inventory," *HVAC&R Research*, vol. 10, no. 2, pp. 153–178, 2004.
- [11] A. Talukdar and A. Patra, "Dynamic model-based fault tolerant control of variable air volume air conditioning system," *HVAC&R Research*, vol. 16, no. 2, pp. 233–254, 2010.
- [12] S. C. Benga, P. Li, S. Sarkar, S. Vichik, V. Adetola, K. Kang, T. Lovett, F. Leonardi, and A. D. Kelman, "Fault-tolerant optimal control of a building hvac system," *Science and Technology for the Built Environment*, vol. 21, no. 6, pp. 734–751, 2015.
- [13] V. Gunes, S. Peter, and T. Givargis, "Improving energy efficiency and thermal comfort of smart buildings with hvac systems in the presence of sensor faults," in *2015 IEEE 17th International Conference on High Performance Computing and Communications, 2015 IEEE 7th International Symposium on Cyberspace Safety and Security, and 2015 IEEE 12th International Conference on Embedded Software and Systems*. IEEE, 2015, pp. 945–950.
- [14] P. M. Papadopoulos, V. Reppa, M. M. Polycarpou, and C. G. Panayiotou, "Distributed design of sensor fault-tolerant control for preserving comfortable indoor conditions in buildings," *IFAC-PapersOnLine*, vol. 51, no. 24, pp. 688–695, 2018.
- [15] M. Maasoumy, A. Pinto, and A. Sangiovanni-Vincentelli, "Model-based hierarchical optimal control design for hvac systems," in *Dynamic Systems and Control Conference*, vol. 54754, 2011, pp. 271–278.
- [16] M. Toub, C. R. Reddy, M. Razmara, M. Shahbakhti, R. D. Robinett III, and G. Aniba, "Model-based predictive control for optimal microcsp operation integrated with building hvac systems," *Energy Conversion and Management*, vol. 199, p. 111924, 2019.
- [17] D. B. Crawley, L. K. Lawrie, C. O. Pedersen, and F. C. Winkelmann, "Energy plus: energy simulation program," *ASHRAE journal*, vol. 42, no. 4, pp. 49–56, 2000.
- [18] S. Salakij, N. Yu, S. Paolucci, and P. Antsaklis, "Model-based predictive control for building energy management. i: Energy modeling and optimal control," *Energy and Buildings*, vol. 133, pp. 345–358, 2016.
- [19] Q. Xu and S. Dubljevic, "Model predictive control of solar thermal system with borehole seasonal storage," *Computers & Chemical Engineering*, vol. 101, pp. 59–72, 2017.
- [20] T. Wei, Y. Wang, and Q. Zhu, "Deep reinforcement learning for building hvac control," in *Proceedings of the 54th annual design automation conference 2017*, 2017, pp. 1–6.
- [21] Z. Zhang, A. Chong, Y. Pan, C. Zhang, S. Lu, and K. P. Lam, "A deep reinforcement learning approach to using whole building energy

- model for hvac optimal control,” in *2018 Building Performance Analysis Conference and SimBuild*, vol. 3, 2018, pp. 22–23.
- [22] G. Gao, J. Li, and Y. Wen, “Deepcomfort: Energy-efficient thermal comfort control in buildings via reinforcement learning,” *IEEE Internet of Things Journal*, vol. 7, no. 9, pp. 8472–8484, 2020.
  - [23] A. Naug, I. Ahmed, and G. Biswas, “Online energy management in commercial buildings using deep reinforcement learning,” in *2019 IEEE International Conference on Smart Computing (SMARTCOMP)*. IEEE, 2019, pp. 249–257.
  - [24] J. Li, W. Zhang, G. Gao, Y. Wen, G. Jin, and G. Christopoulos, “Towards intelligent multi-zone thermal control with multi-agent deep reinforcement learning,” *IEEE Internet of Things Journal*, 2021.
  - [25] Z. Du, B. Fan, J. Chi, and X. Jin, “Sensor fault detection and its efficiency analysis in air handling unit using the combined neural networks,” *Energy and Buildings*, vol. 72, pp. 157–166, 2014.
  - [26] J. Liu, M. Zhang, H. Wang, W. Zhao, and Y. Liu, “Sensor fault detection and diagnosis method for ahu using 1-d cnn and clustering analysis,” *Computational intelligence and neuroscience*, vol. 2019, 2019.
  - [27] M. S. Mirnaghi and F. Haghighat, “Fault detection and diagnosis of large-scale hvac systems in buildings using data-driven methods: A comprehensive review,” *Energy and Buildings*, p. 110492, 2020.
  - [28] V. Reppa, P. Papadopoulos, M. M. Polycarpou, and C. G. Panayiotou, “A distributed architecture for hvac sensor fault detection and isolation,” *IEEE Transactions on Control Systems Technology*, vol. 23, no. 4, pp. 1323–1337, 2014.
  - [29] Z.-H. Zhou, “A brief introduction to weakly supervised learning,” *National science review*, vol. 5, no. 1, pp. 44–53, 2018.
  - [30] Y.-Y. Sun, Y. Zhang, and Z.-H. Zhou, “Multi-label learning with weak label,” in *Proceedings of the AAAI Conference on Artificial Intelligence*, vol. 24, no. 1, 2010.
  - [31] G. Papandreou, L.-C. Chen, K. P. Murphy, and A. L. Yuille, “Weakly-and semi-supervised learning of a deep convolutional network for semantic image segmentation,” in *Proceedings of the IEEE international conference on computer vision*, 2015, pp. 1742–1750.
  - [32] X. Zhu and A. B. Goldberg, “Introduction to semi-supervised learning,” *Synthesis lectures on artificial intelligence and machine learning*, vol. 3, no. 1, pp. 1–130, 2009.
  - [33] T. Chen, S. Kornblith, M. Norouzi, and G. Hinton, “A simple framework for contrastive learning of visual representations,” in *International conference on machine learning*. PMLR, 2020, pp. 1597–1607.
  - [34] G. Hinton, O. Vinyals, and J. Dean, “Distilling the knowledge in a neural network,” *arXiv preprint arXiv:1503.02531*, 2015.
  - [35] Y. Kim and A. M. Rush, “Sequence-level knowledge distillation,” *arXiv preprint arXiv:1606.07947*, 2016.
  - [36] S. Xu, Y. Wang, Y. Wang, Z. O’Neill, and Q. Zhu, “One for many: Transfer learning for building hvac control,” in *Proceedings of the 7th ACM International Conference on Systems for Energy-Efficient Buildings, Cities, and Transportation*, 2020, pp. 230–239.
  - [37] Y. Chen, Z. Tong, Y. Zheng, H. Samuelson, and L. Norford, “Transfer learning with deep neural networks for model predictive control of hvac and natural ventilation in smart buildings,” *Journal of Cleaner Production*, vol. 254, p. 119866, 2020.
  - [38] P. Lissa, M. Schukat, and E. Barrett, “Transfer learning applied to reinforcement learning-based hvac control,” *SN Computer Science*, vol. 1, 2020.
  - [39] D. P. Kingma and J. Ba, “Adam: A method for stochastic optimization,” *arXiv preprint arXiv:1412.6980*, 2014.
  - [40] M. Wetter, “Co-simulation of building energy and control systems with the building controls virtual test bed,” *Journal of Building Performance Simulation*, vol. 4, no. 3, pp. 185–203, 2011.
  - [41] S. Wilcox and W. Marion, “Users manual for tmy3 data sets,” 2008.